ELSEVIER

Polymer 40 (1999) 4929–4940

polymer

Investigations of some selected properties of electrochemically synthesized poly(*N*-ethyl aniline) films

Anjali A. Athawale*, Somaji F. Patil, Bhavana Deore

Department of Chemistry, University of Pune, Pune 411007, India

Received 7 November 1997; received in revised form 30 March 1998; accepted 29 September 1998

Abstract

The optical, morphological, thermal and redox properties of galvanostatically deposited poly(*N*-ethyl aniline) films are investigated. Effects of monomer concentration and substrate resistance on film properties have been reported. At higher concentration (0.8 and 1.0 M), the formation of a conducting phase with an absorbance maxima at ~ 840 nm is found to be more predominant. The substrate resistance also has a profound influence on the film properties in terms of rate and selectivity in deposition of the conducting phase. These results are supported by IR spectroscopy. The redox properties are affected by concentration of monomer while the substrate resistance contributes towards loss in reversibility of the species formed, especially at higher monomer concentration. Also, the morphology of the films exhibits improvement in quality with monomer concentration. The density of the fibres is affected by the decrease in substrate resistance. Thermal pattern also exhibits variation in terms of the number of steps involved in decomposition as well as the final decomposition temperature.

Keywords: *N*-ethyl aniline; Monomer concentration; Sheet resistance

1. Introduction

Conductive electroactive polymers [1,2] are known to exhibit intriguing electrical, electrochemical, and optical properties which have led to applications in various fields such as display devices [3,4], microelectronics [5], light weight batteries [6,7], antistatic coatings and gas sensors [8]. Polyaniline is one of the members of this class of polymers. However, in certain applications the substituted derivatives are found to have better candidature due to their flexibility in chemical properties in comparison with polyaniline. Some literature is available which accounts for the various properties of substituted derivatives [9–13]. In this respect, the ring substituted anilines have been studied extensively. However, less attention has been paid towards the *N*-substituted derivatives of aniline [14–18]. Hence, one needs to explore these materials so as to control their physical and chemical behaviour before utilizing them for large scale applications.

In the present work, efforts have been made to study the influence of monomer concentration and substrate resistance on electrochemically synthesized poly(*N*-ethyl aniline) films. The films have been examined using various techniques such as UV-Vis and IR spectroscopy, cyclic voltammetry, scanning electron microscopy and thermogravimetry.

2. Experimental

A.R. grade chemicals were used for the experimental work. Different concentrations of monomer (0.4, 0.6, 0.8 and 1.0 M) were prepared in 1.0 M HCl (doubly distilled water) by adding the appropriate amount of *N*-ethyl aniline. The electrochemical cell used for the polymerization comprised of SnO_2:F coated glass (2.5×1 cm^2) as the working electrode, platinum as auxiliary electrode and SCE as the reference electrode. SnO_2:F films deposited on a corning glass substrate with two different sheet resistances (10 and 50 Ω cm^{-1}) were prepared by spray pyrolysis [19]. The polymer films were deposited under galvanostatic conditions at a current strength of 0.5 mA using a potentiostat/galvanostat (Elico CL 95). The film was deposited for a period of 2 h at 0.4 and 0.6 M *N*-ethyl aniline concentrations and 1 h at 0.8 and 1.0 M concentrations. Deposited films were washed with distilled water, dried and then utilized for characterization. An Hitachi 220 UV-Vis double beam spectrophotometer was used for recording the optical spectra. FT-IR spectra were recorded on a Perkin Elmer (Model

* Corresponding author. Fax: +0091-212-353899.
E-mail address: agbed@chem.unipune.ernet.in (A.A. Athawale)

0032-3861/99/$ - see front matter
PII: S0032-3861(98)00695-8

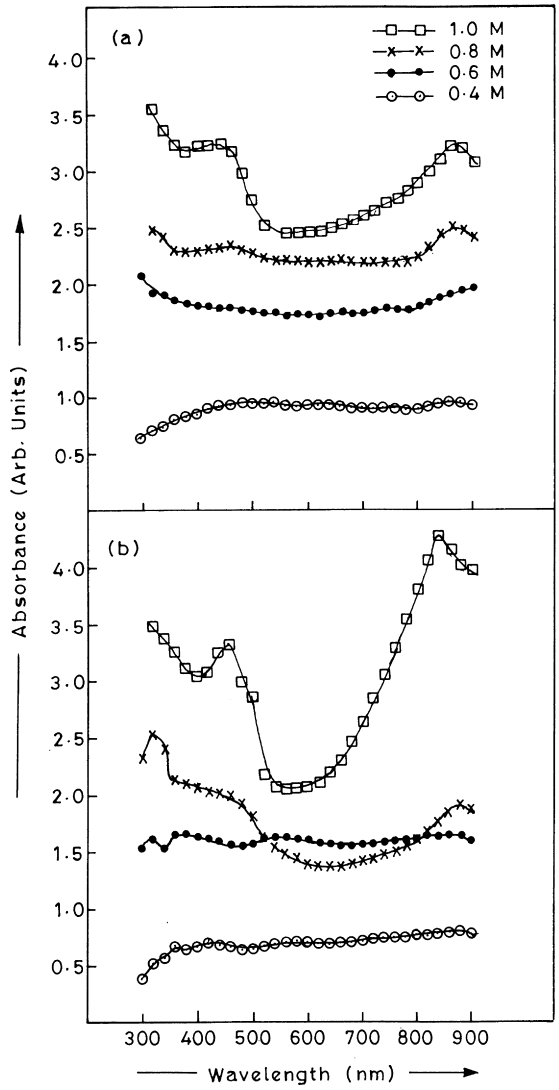

Fig. 1. UV-visible absorption spectra of poly(*N*-ethyl aniline) films deposited as a function of monomer concentration. (Substrate resistance (a) 10 Ω cm^{-1} and (b) 50 Ω cm^{-1}.)

1600) FT-IR spectrophotometer in the range of 400–4000 cm^{-1}. The samples were scraped from the SnO_2:F electrode and prepared in pellet form using KBr. Cyclic voltammetric studies were performed using a potentiostat (Cypress Model, Omni 90). The dimension of the SnO_2:F glass electrode was 10 × 3 mm and the polymer was deposited in a 3 × 3 mm area. The potential was cycled between − 0.2 to 1.2 V versus SCE at a scan rate of 100 mV/s. The morphological features were examined using a Cambridge Instruments stereoscan S 120 scanning electron microscope (SEM). Before exposure to SEM the films were coated with a thin layer of gold (thickness ~ 20 nm) using a Bio Rad E 5000 sputter coater unit. Thermograms of the polymer were recorded on a thermogravimetric analyzer (Perkin Elmer, Model TGA-7) in an O_2 atmosphere at a scanning rate of 10°C/min.

3. Results and discussion

The UV-Visible spectra of poly(*N*-ethyl aniline) films deposited as a function of monomer concentration on substrates with a sheet resistance of 10 and 50 Ω cm^{-1} are given in Fig. 1. The magnitude of absorbance shows an increasing trend on going from 0.4 to 1.0 M monomer concentration. It is worth noting that a minimum concentration of ~ 0.4 M of *N*-ethyl aniline is needed at which polymerization takes place yielding films with measurable absorbance. As seen in Fig. 1, the spectra after electrochemical oxidation of 0.4 and 0.6 M *N*-ethyl aniline on both types of substrates are broad in nature. On the other hand, at higher monomer concentrations of 0.8 and 1.0 M the spectra shows a sharp peak corresponding to the conducting emeraldine phase (delocalized polaron/bipolaron transition). The degree of selectivity in the formation of conductive phase is greater in the case of films deposited on substrate with sheet resistance of 50 Ω cm^{-1}. The other peaks appear ~ 320 and 420 nm, respectively, representing the formation of leucoemeraldine phase ($\pi-\pi^*$ transition) and radical cations (polarons) [20,21].

These results can be explained on the basis of the varying rate of reaction as well as the competitive products formed during deposition. At 0.4 and 0.6 M monomer concentration the polymerization reaction is hindered strongly due to the formation of a large fraction of benzidines via a nitrene cation intermediate [22]. The nitrene cations having sufficiently long lifetime are formed more preferably in highly acidic medium and low monomer concentration. These are later attacked by other monomer molecules and nucleophiles present in the solution thereby giving benzidines as the major product. Apart from this, it is obvious that the tail to tail coupling of the molecules would be a more favoured reaction rather than head to tail or head to head coupling in *N*-ethyl aniline as a result of steric hindrance caused by the bulky ethyl group.

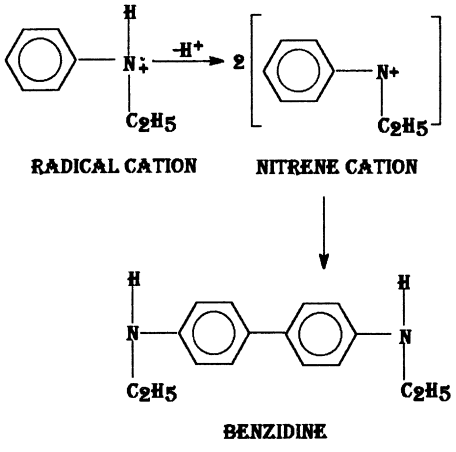

When the monomer concentration is increased to 0.8 and 1.0 M the rate of reaction is expected to increase since the collision of molecules would take place at a faster rate in

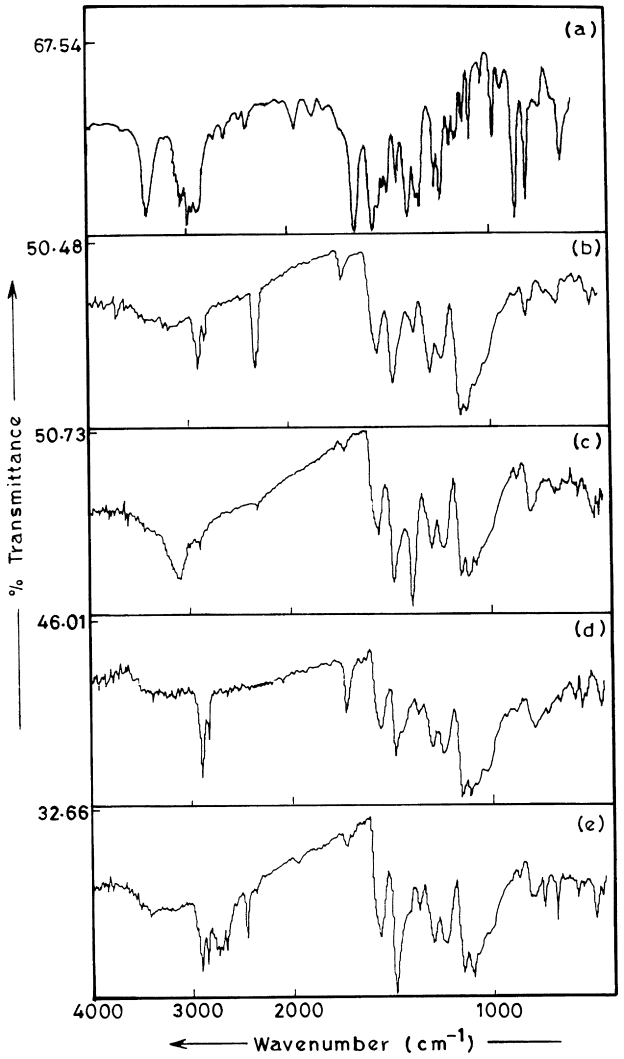

Fig. 2. FT-IR absorption spectra of monomer (a) and poly(*N*-ethyl aniline) films deposited at different monomer concentrations. ((b) 0.4 M and (c) 1.0 M on 10 Ω cm^{-1} substrate and (d) 0.4 M and (e) 1.0 M on 50 Ω cm^{-1} substrate.)

such a medium. Furthermore, there is an appreciable decrease in the concentration of nitrene cation and hence, benzidines. Instead, predominantly radical cations are formed, followed by polymerization. The higher degree of selectivity in the formation of conducting phase in the film deposited on substrate with sheet resistance of 50 Ω cm^{-1} in comparison with that deposited on 10 Ω cm^{-1} substrate can be attributed to the optimum rate of deposition contributing towards the efficient conversion of pernigraniline to emeraldine salt [23].

Fig. 2a and Fig. 2b–e represent the FT-IR spectra of *N*-ethyl aniline together with the poly(*N*-ethyl aniline) films deposited on substrates with sheet resistance of 10 and 50 Ω cm^{-1} at 0.4 and 1.0 M monomer concentrations. A comparison of the spectra of the polymer with that of the monomer reveals the presence of two strong bands ~ 749 and 692 cm^{-1} in the monomer spectra corresponding to the terminal phenyl group [24]. The intensity of the above two bands is drastically reduced in the polymer spectra, contrary to this, an intense band is observed ~ 820 cm^{-1} which is characteristic of the paradisubstituted aromatic ring through which polymerization proceeds [25]. Further, the polymer shows two intense peaks ~ 1120 and ~ 620 cm^{-1} representing the in-plane and out-of-plane C–H bending motion of quinoid and benzenoid rings [26]. The C–N stretching bands which are characteristic of an aromatic amine are observed in the region of 1230 and 1350 cm^{-1}. The peak ~ 1314 cm^{-1} corresponds to aromatic $C–N^+$ stretching while the C–N stretching of secondary amine is represented by the peak ~ 1230 cm^{-1} [26]. In the C–H stretching region the aromatic C–H is easily identified at ~2923 cm^{-1} [27]. Bands at ~ 1500 and ~ 1600 cm^{-1} are assigned to the non-symmetric C_6 ring stretching modes. The higher frequency vibration has a major contribution from the quinoid rings, while the lower frequency mode depicts the presence of benzenoid ring units. The relative intensity of these bands points towards the oxidation state of the material [25–28]. In addition to this, the presence of both these bands clearly shows that the polymer is composed of amine and imine units. Furthermore, it gives support to the earlier prediction for the presence of different oxidation states of the polymer.

At higher monomer concentration and substrate with sheet resistance of 50 Ω cm^{-1} the higher relative intensity ratio of quinoid to benzenoid ring modes [$|_{\sim 1600}/|_{\sim 1500}$] of ~ 1.29 can be attributed to the predominant formation of conducting reduced phase. On the other hand, at lower monomer concentrations and substrates with sheet resistance of 10 and 50 Ω cm^{-1} the ratio is found to be ~1.02. This can be attributed to a large contribution of quinoid pertaining to the higher oxidized phase.

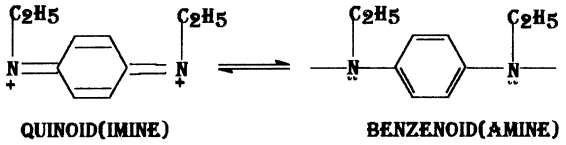

The redox properties of poly(*N*-ethyl aniline) were investigated using cyclic voltammetry (CV) as a function of monomer concentration on substrates with sheet resistance of 10 and 50 Ω cm^{-1}. The effect of monomer concentration on the voltammetric features of *N*-ethyl aniline on substrates with sheet resistance of 10 Ω cm^{-1} are depicted in Fig. 3. Optimum scan rate for the polymerization process has been determined by varying the scan rate. Fig. 3 shows the presence of two reversible redox couples ~ 0.42 and 0.52 V along with an additional cathodic peak ~ 0.31 V. The peak ~ 0.31 V is related to the oxidation of nitrogen atom of the monomer molecule, i.e., formation of polaron as proposed by the electrochemical reaction mechanism for substituted polyanilines [29]. The couple ~ 0.42 V is assigned to the formation of emeraldine salt (head to tail coupling) together with soluble benzidine derivatives (tail to

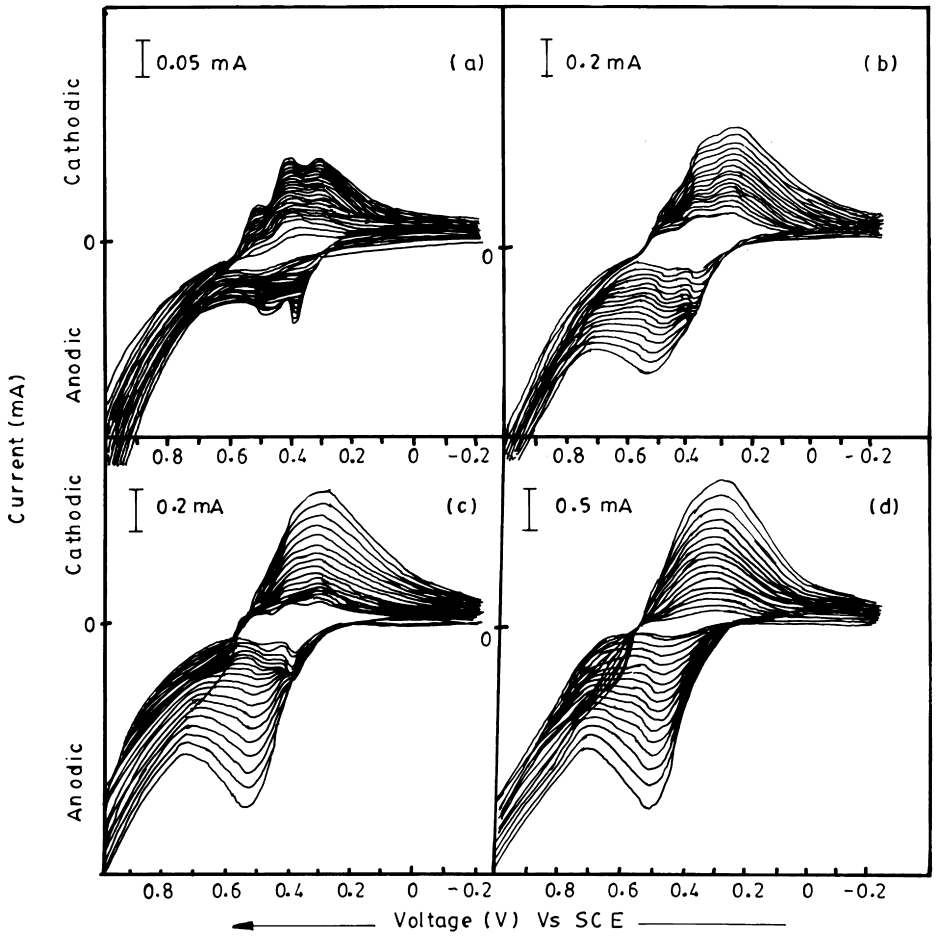

Fig. 3. Cyclic voltammograms of *N*-ethyl aniline recorded as a function of monomer concentration. ((a) 0.4 M, (b) 0.6 M, (c) 0.8 M and (d) 1.0 M, substrate resistance 10 $\Omega\ cm^{-1}$.)

tail coupling). The presence of hydrolysis products benzoquinone/hydroquinone couple is associated with the peak $\sim$ 0.52 V [30]. The benzoquinone thus formed is solubilized partly in the reaction vessel while the remainder is adsorbed on the electrode surface. Presence of an anodic peak $\sim$ 0.65 V associated with a diradical dication is more distinctly observed in the presence of 0.8 and 1.0 M monomer concentration [29]. The huge, irreversible oxidation peak $\sim$ 0.9 V represents the polymer growth. The anodic peak $\sim$ 0.42 V is seen to disappear with increasing monomer concentration. At a concentration of 0.4 M the peaks are well distinguished and reversible. With increase in concentration from 0.6 to 1.0 M, loss in reversibility is observed, however, magnitude of the current is seen to be enhanced.

On comparing the cyclic voltammograms of poly(*N*-ethyl aniline) with polyaniline [31] a significant shift ($\sim$ 0.1 V) is observed in the peak position of the radical cation. The shift in peak potential to a higher value in poly(*N*-ethyl aniline) arises due to the steric hindrance caused by the bulky ethyl group present on the nitrogen atom in the monomer. The second peak for the hydrolysis product, i.e. benzoquinione, is also affected suggesting that the mechanism involved in the formation of this species is influenced by the position of substituent. The above fact is confirmed by the differences in the magnitude of current in the two species, whereby polyaniline exhibits a current magnitude almost 10 times greater than that for poly(*N*-ethyl aniline). This in turn proves the faster rate of reaction and formation of a greater fraction of conducting phase in polyaniline than poly(*N*-ethyl aniline).

The redox properties are seen to strongly depend on the reaction rate prevailing during polymerization. The fact that the reaction rate in poly(*N*-ethyl aniline) is expected to be lower in comparison with polyaniline and other substituted derivatives such as poly(*o*-anisidine), poly(*o*-toluidine) [23, 32] etc. is confirmed from the range of monomer concentrations at which this polymer is obtained. At 0.4 and 0.6 M concentrations, the rate of reaction being relatively slower, the fraction of monomers available for autocatalysis mechanism [22] would be less since a part of them would be utilized for generating competitive reaction products, hence, a small shoulder is observed at $\sim$ 0.65 V. In contrast to this, the reaction rate is accelerated at higher monomer concentrations simultaneous to inhibition in the formation of benzidines. As a result, the formation of diradical dication is expected to take place in the initial stages, favouring the polymer growth. The

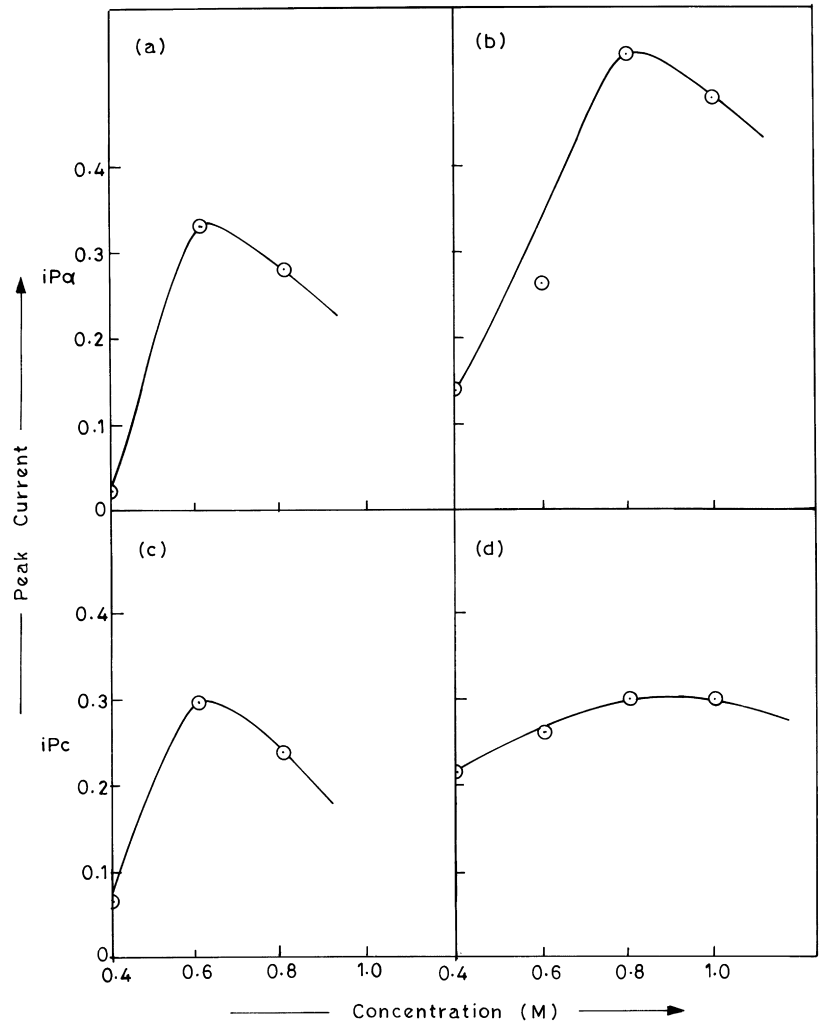

Fig. 4. Plot of ip_a and ip_c versus monomer concentration at peak potential of ~ 0.42 V. (ip_a = Substrate resistance = (a) 10 Ω cm^{-1} and (b) 50 Ω cm^{-1}. ip_c = Substrate resistance = (c) 10 Ω cm^{-1} and (d) 50 Ω cm^{-1}.)

plot of ip_a and ip_c (~ 0.42 V) versus monomer concentration as shown in Fig. 4 supports the above explanation. It shows an increase in peak current up to 0.6 M in the case of CV taken on substrates with sheet resistance of 50 Ω cm^{-1}, while the peak ~ 0.42 V is absent in the CV obtained on substrates with sheet resistance of 10 Ω cm^{-1}.

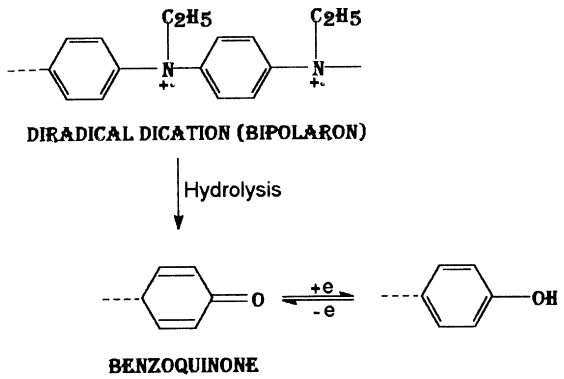

Another significant parameter of interest is the influence of sheet resistance of the substrate on the polymerization process, especially at higher monomer concentrations (Fig. 5). At lower concentrations, the cyclic voltammograms exhibit differences in the rate of polymer deposition in terms of the magnitude of all the peak currents when a comparison is made between substrates with sheet resistance of 10 and 50 Ω cm^{-1} [19,33]. However, at 1.0 M concentration the cyclic voltammograms recorded on substrates with sheet resistance of 50 Ω cm^{-1} show a drastic shift in anodic peak potential ~ 0.54 V (~ 20 mV at the 2nd cycle to 110 mV at the 12th cycle) whereas saturation is observed at the cathodic side. This distortion with loss in reversibility is due to a combined effect of ohmic drop associated with the monomer concentration and sheet resistance of the substrate.

Fig. 6 represents the cyclic voltammograms taken at various scan rates between 25–200 mV/s at two extreme concentrations of 0.4 and 1.0 M on substrates with sheet resistance of 10 and 50 Ω cm^{-1}. The reversibility of peak

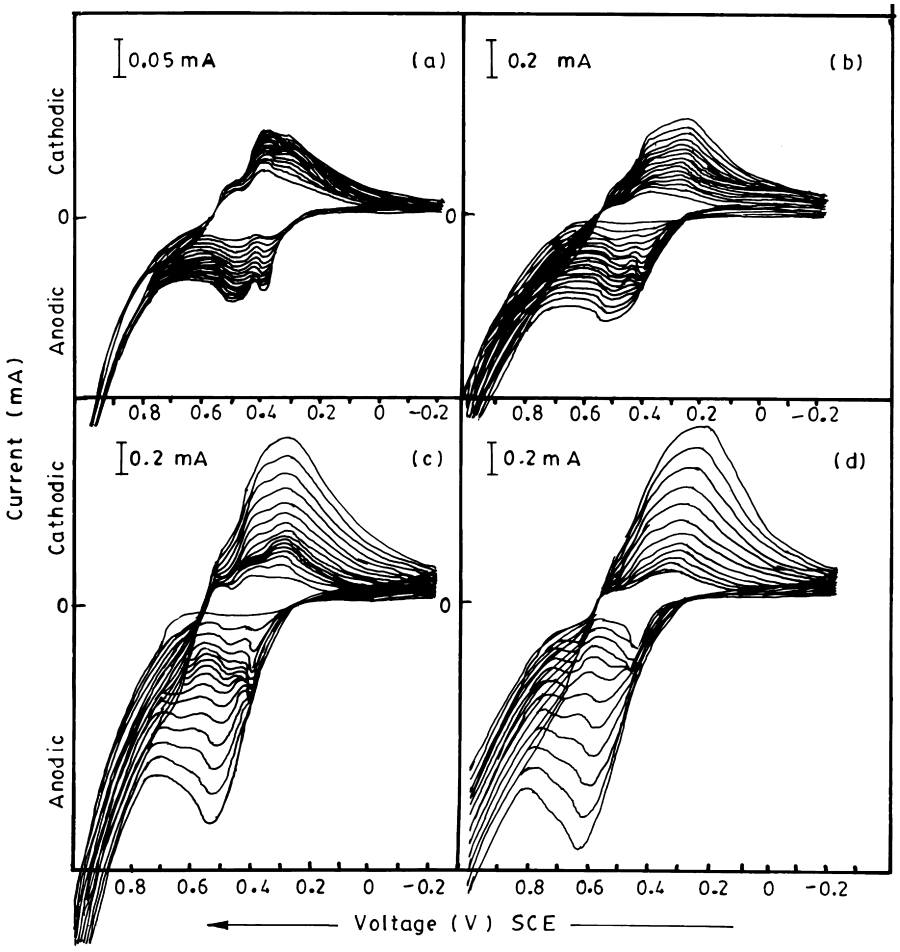

Fig. 5. Cyclic voltammograms of *N*-ethyl aniline recorded as a function of monomer concentration. ((a) 0.4 M, (b) 0.6 M, (c) 0.8 M and (d) 1.0 M, substrate resistance 50 $\Omega\ cm^{-1}$.)

is seen to diminish as a function of scan rate. The redox couples are clearly seen up to a scan rate of 125 mV/s. However, a further increase in the scan rate leads to a distortion in the cyclic voltammograms which might be due to an increase in the thickness of polymer film along with a large contribution of non-faradaic current.

The scanning electron micrographs of the deposited films (Fig. 7 and Fig. 8) reveal differences in patterning with concentration of monomer. Density, as well as quality of the film, is observed to improve with increasing monomer concentration and decreasing sheet resistance of substrate. At 0.4 and 0.6 M concentration the morphology shows coral-like growth (Figs. 7 and 8a and b) bearing three dimensions. The overall development of the structure is seen to take place through joining up of small tiny fibrils which are formed at the earlier stages of deposition at specific nucleation centers. The nucleation centers are nothing but the grain boundaries of the SnO_2:F lattice [32,34]. On increasing the monomer concentration to 0.8 M the presence of thin long fibres is distinctly observed (Figs. 7 and 8c). However, the film deposited on substrates with sheet resistance of 10 $\Omega\ cm^{-1}$ demonstrates a purely fibrillar nature, the fibres are seen to be bunched together which must be the nucleation zone. On the other hand, on substrates with sheet resistance of 50 $\Omega\ cm^{-1}$, it is noted that long thin fibres are grown on the upper surface below which are present islands interconnected to each other. Further increase in concentration to 1.0 M results in a still different kind of morphology. The morphology gives the appearance of two dimensions comprised of closely spaced flat islands. The growth is seen to progress in a layer-by-layer fashion (Figs. 7 and 8d).

These results can be attributed to the varying rate of deposition as a function of concentration of monomer together with the sheet resistance of the substrate. Quality of film exhibits an improvement at higher concentrations since the formation of competitive products is eliminated completely.

Similar to the above-mentioned properties, the thermal properties of the film also seem to vary with monomer concentration and sheet resistance of substrate. Fig. 9 depicts the thermograms of poly(*N*-ethyl aniline) films

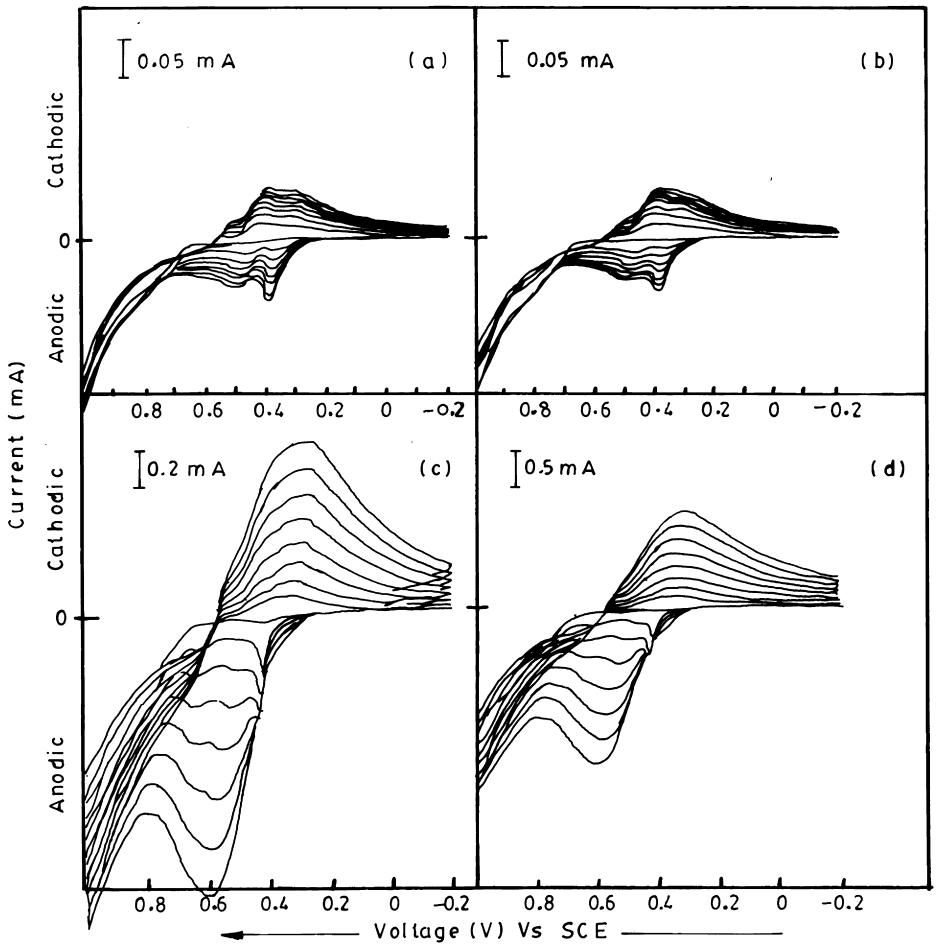

Fig. 6. Cyclic voltammograms of *N*-ethyl aniline recorded as a function of scan rate 25–200 mV. (Substrate resistance 10 $\Omega\ cm^{-1}$ = (a) 0.4 M and (c) 1.0 M and 50 $\Omega\ cm^{-1}$ = (b) 0.4 M and (d) 1.0 M.)

deposited at 0.4 and 1.0 M concentration on substrates with sheet resistance of 10 and 50 $\Omega\ cm^{-1}$. The weight losses taking place in individual steps and the corresponding temperature ranges are given in Table 1. From the table, it appears that at lower monomer concentration the films deposited on both types of substrates show a similar nature except for minor changes in the individual weight losses. Contrary to this, a significant difference in weight loss (1st step) is observed at higher monomer concentration when compared to substrates with sheet resistance of 10 and 50 $\Omega\ cm^{-1}$. These results are in agreement with the optical spectra discussed earlier. At lower monomer concentration the thermograms demonstrate a four-step decomposition pattern while at higher monomer concentration the polymer undergoes decomposition in three steps [35]. The loss observed (0.4 M) in the 1st, 2nd and 3rd steps is attributed to the loss of water molecules along with volatilization of Cl^- as HCl or Cl_2, loss of substituted groups and low molecular weight fragments followed by breakdown and degradation of polymer matrix. In the presence of 0.4 M monomer concentration, mixed phases are formed and a broad distribution of molecular fragments could be possible. Due to this, the intermediate step is split into two. At higher monomer concentration a greater fraction is lost in the 1st step in the case of films obtained on substrate with sheet resistance of 50 $\Omega\ cm^{-1}$, since the fraction of conducting phase formed is greater in this case than the film deposited on substrate with sheet resistance of 10 $\Omega\ cm^{-1}$. Also, the negative shift in the final decomposition temperature with monomer concentration arises due to greater fraction of conducting phase.

4. Conclusion

Quality of the film and selectivity in the formation of conducting phase is found to be enhanced in the presence of higher monomer concentration and sheet resistance of substrate.

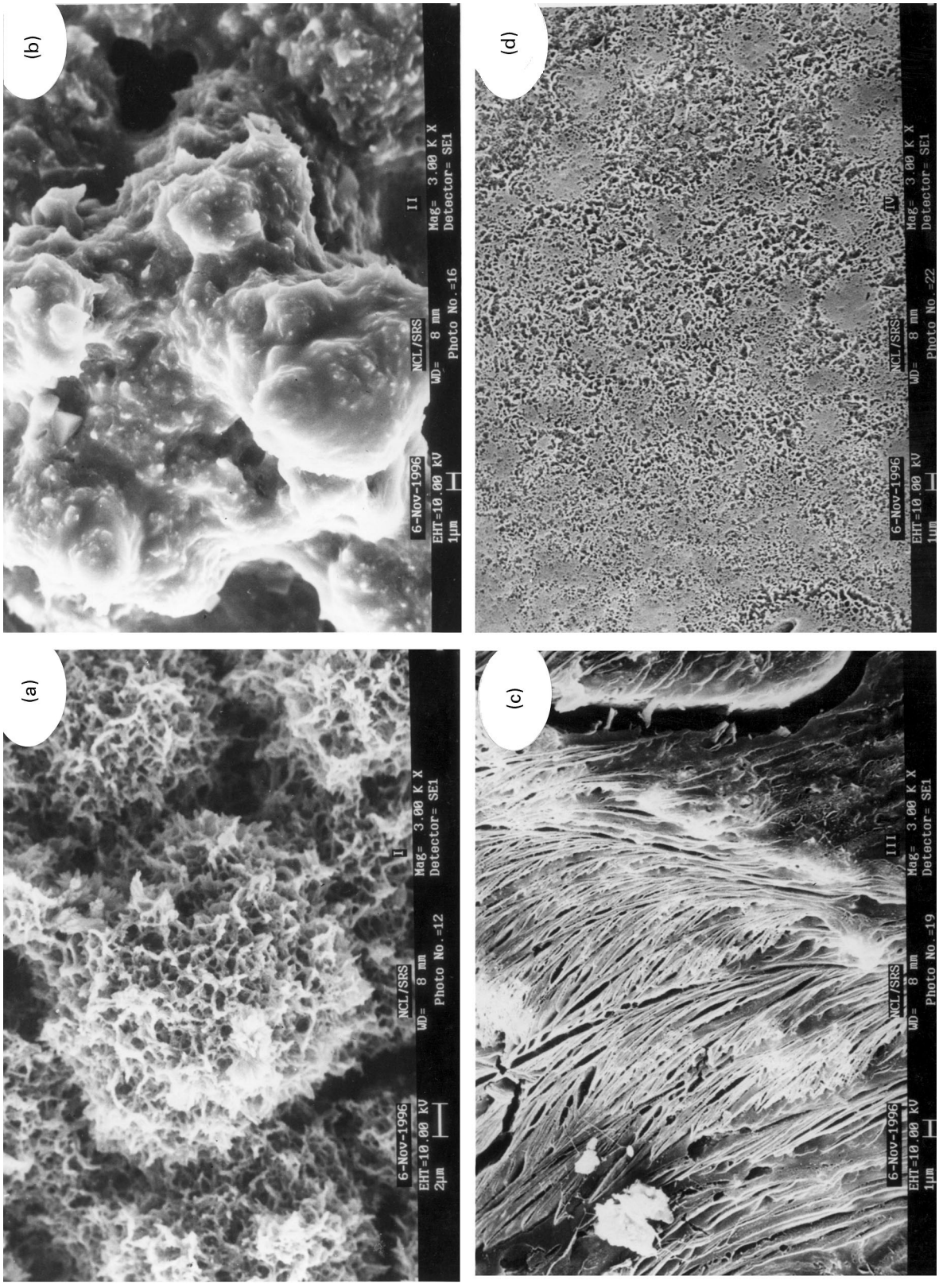

Fig. 7. Scanning electron micrographs of poly(*N*-ethyl aniline) films deposited as a function of monomer concentration. ((a) 0.4 M, (b) 0.6 M, (c) 0.8 M and (d) 1.0 M, substrate resistance 10 Ω cm^{-1}.)

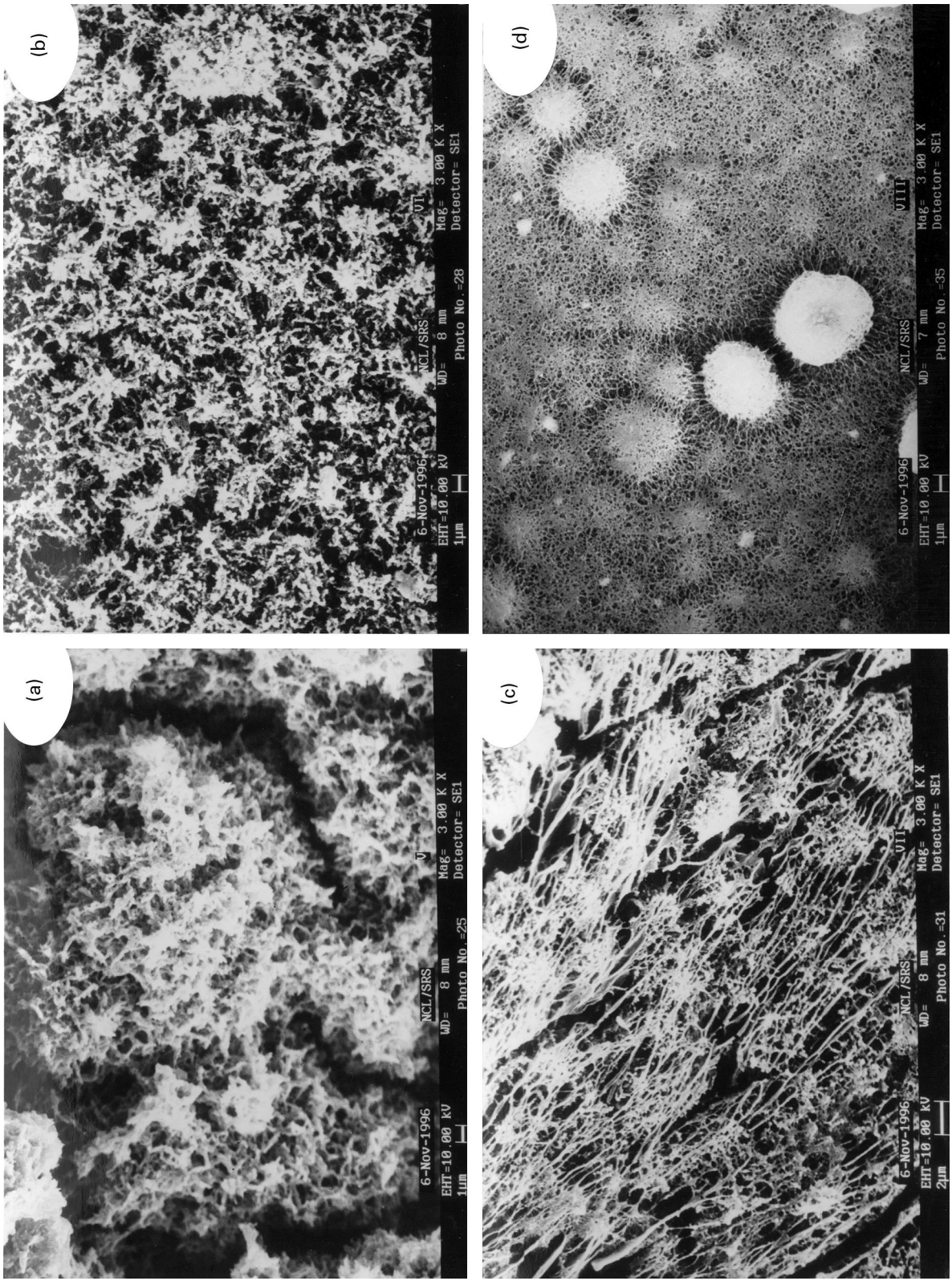

Fig. 8. Scanning electron micrographs of poly(*N*-ethyl aniline) films deposited as a function of monomer concentration. ((a) 0.4 M, (b) 0.6 M, (c) 0.8 M and (d) 1.0 M, substrate resistance 50 $\Omega\,cm^{-1}$.)

Table 1
Weight losses of individual steps of poly(*N*-ethyl aniline) films with respect to temperature ranges

Temperature °C	Steps	0.4 M 10 Ω cm^{-1} % wt loss	0.4 M 50 Ω cm^{-1} % wt loss	Temperature °C	Steps	1.0 M 10 Ω cm^{-1} % wt loss	1.0 M 50 Ω cm^{-1} % wt loss
50–150	1st	15.17	11.72	50–250	1st	34.81	54.47
150–280	2nd	18.62	22.06	250–550	2nd	16.89	22.06
280–550	3rd	22.75	26.20	550–850[a]	3rd	48.30	24.47
550–900	4th	43.45	40.02	550–870[b]			

[a] = 10 Ω cm^{-1}.
[b] = 50 Ω cm^{-1}.

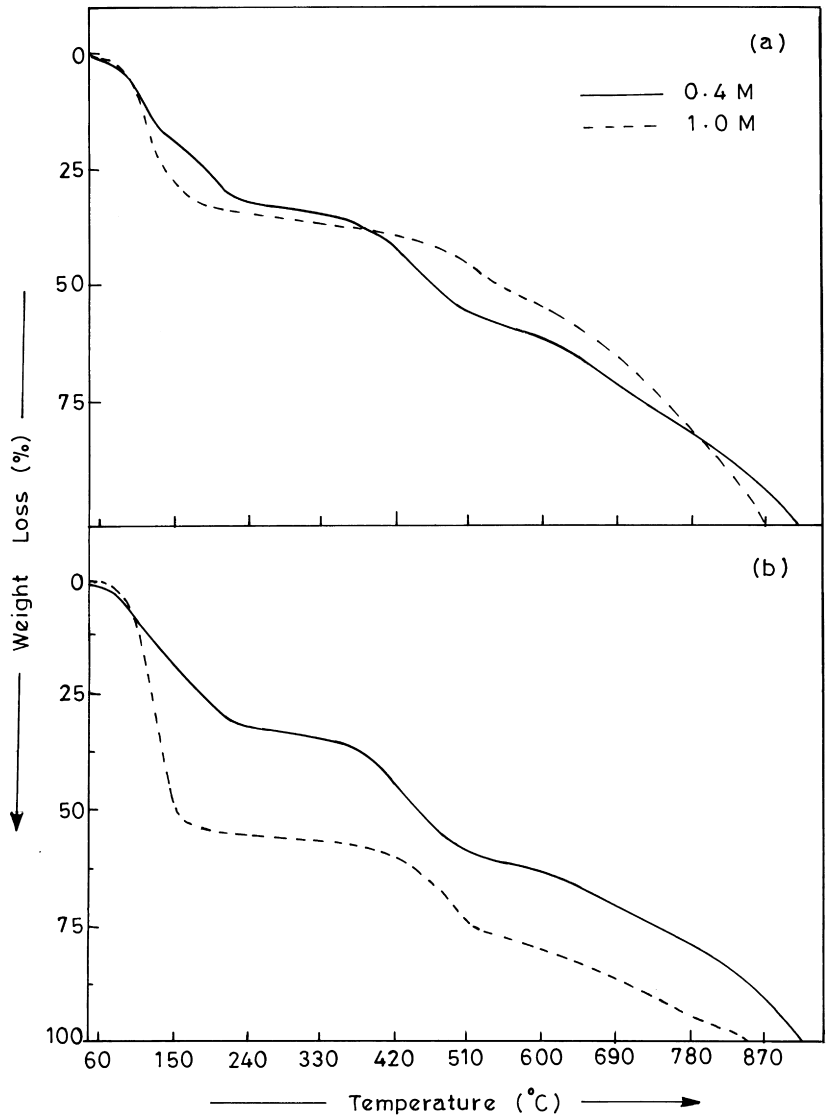

Fig. 9. Thermograms of poly(*N*-ethyl aniline) films deposited at different monomer concentrations. (Substrate resistance = (a) 10 Ω cm^{-1} and (b) 50 Ω cm^{-1}.)

Acknowledgements

The authors, AAA and SFP acknowledge the support of this research by DST. One of the authors, Ms. Bhavana Deore, is thankful to CSIR for providing financial assistance.

References

[1] Kanatzidis G. Chem Eng News 30 December 1990.
[2] Roth S, Graupher W. Synth Met 1993;53-57:3623.
[3] Akhtar M, Weakliem HA, Paiste RM, Gaughan K. Synth Met 1988;26:103.
[4] Nguyen MT, Dao LH. J Electrochem Soc 1989;136:2131.
[5] Paul EW, Ricco AJ, Wrighton MS. J Phys Chem 1985;89:1441.
[6] Skotheim TA. Handbook of conducting polymers, Vols. 1 and 2. New York: Marcel Dekker, 1986.
[7] Santhanam K, Gupta N. Polymer Sci 1993;1(9):284.
[8] Shinohara H, Chiba T, Aizawa M. Sensors and Actuators 1989;13:79.
[9] Aparno GD, Leclerc M, Zotti G. J Electroanal Chem 1993;351:145.
[10] Mortimer RJ. Mater Chem 1995;5:969.
[11] Dao LH, Leclerc M, Guay J, Chevalier JW. Synth Met 1989;29:E377.
[12] Leger JM, Beden B, Lamy C, Ocon P, Sierio C. Synth Met 1994;62:9.
[13] Anand J, Palaniappan S, Sathyanarayana DN. Synth Met 1994;66:129.
[14] MacDiarmid AG. Faraday Discuss Chem Soc 1989;88:317.
[15] Ye S, Benser S, Dao LH, Vish AJ. J Electroanalytical Chem 1995;71:381.
[16] Leclerc M, Guay J, Dao LH. Macromolecules 1989;22:649.
[17] Aparno GD, Leclerc M, Zotti G. Macromolecules 1992;25:2145.
[18] Zheng WY, Levon K, Laakso J, Osterholm J. Macromolecules 1994;27:7754.
[19] Agashe C, Takawale MG, Marathe BR, Bhide VG. Sol Energ Mater 1988;17:99.
[20] Lu FL, Wudl F, Nowak M, Heeger AJ. J Am Chem Soc 1986;108:8311–8313.
[21] Huang WS, MacDiarmid AG. Polymer 1993;34(9):1833–1843.
[22] Shim YB, Won M, Park SM. J Electrochem Soc 1990;137(2):538–544.
[23] Bedekar AG, Patil SF, Patil RC, Agashe C. Mater Chem and Phys 1995;40:1.

[24] Comisso N, Daolio S, Mengoli G, Salmaso R, Zecchin S, Zoth G. J Electroanal Chem 1988;265:97.
[25] Milton AJ, Monkman AP. J Phys D Appl Phys 1993;26:1468.
[26] Bernard MC, Hugot-Le G. J Electrochem Soc 1994;141(10):2682.
[27] Epstein AJ, Macall RP, Ginder JM, MacDiarmid AG. Spectroscopy Advanced Materials 1991;19:355.
[28] Athawale AA, Patil SF, Patil RC, Deore BA, Vijayamohanan K. Polymer Journal 1997;29(10):787.
[29] Stillwell DE, Park SM. J Electrochem Soc 1988;135:2254.
[30] Cui CQ, Ong LH, Tan TC, Lee JY. Electrochim Acta 1993;38:1404.
[31] Bedekar AG, Patil SF, Patil RC, Vijayamohanan K. Mater Chem Phys 1997;48:76.
[32] Bedekar AG, Patil SF, Patil RC, Agashe C. J Phys D Appl Phys 1994;27:1727–1731.
[33] Ocon P, Herrasti P, Vara JM, Vazquez L, Salvarezza RC, Arvia AJ. J Phys Chem 1994;28:2418.
[34] Bedekar AG, Patil SF, Patil RC, Agashe C. Polymer Journal 1995;27(4):319.
[35] Traore MK, Stevenson WTK, McCormick MJ, Dorey MC, Wen S, Meyers D. Synth Met 1991;40:137.